

ChemComm

Accepted Manuscript



This is an *Accepted Manuscript*, which has been through the Royal Society of Chemistry peer review process and has been accepted for publication.

Accepted Manuscripts are published online shortly after acceptance, before technical editing, formatting and proof reading. Using this free service, authors can make their results available to the community, in citable form, before we publish the edited article. We will replace this *Accepted Manuscript* with the edited and formatted *Advance Article* as soon as it is available.

You can find more information about *Accepted Manuscripts* in the [Information for Authors](#).

Please note that technical editing may introduce minor changes to the text and/or graphics, which may alter content. The journal's standard [Terms & Conditions](#) and the [Ethical guidelines](#) still apply. In no event shall the Royal Society of Chemistry be held responsible for any errors or omissions in this *Accepted Manuscript* or any consequences arising from the use of any information it contains.

Cite this: DOI: 10.1039/c0xx00000x

www.rsc.org/xxxxxx

ARTICLE TYPE

Three different metal-organic frameworks derived from one-pot crystallization and their controllable synthesis

Chuan-Lei Zhang,^a Yan-Le Li,^b Ting Wang,^a Ze-Min Ju,^a He-Gen Zheng,^{*a} Jing Ma^{*b}

Received (in XXX, XXX) Xth XXXXXXXXX 20XX, Accepted Xth XXXXXXXXX 20XX

DOI: 10.1039/b000000x

Three different Co-MOFs, $[\text{Co}_3(\text{L})_2(\text{DPDP})]_n$ (**1**), $[\text{Co}(\text{HL})(\text{DPDP})]_n$ (**2**) and $\{[\text{Co}(\text{HL})(1/2\text{DPDP})_3(\text{H}_2\text{O})] \cdot \text{H}_2\text{O}\}_n$ (**3**) ($\text{H}_3\text{L} = 4,4',4''\text{-(nitrilotris(methylene))tribenzoic acid}$, $\text{DPDP} = 4,4'\text{-(2,5-dibutoxy-1,4-phenylene)dipyridine}$) have been co-crystallized in one-pot reaction. Based on the significant differences of three structures, we adopt solvents to regulate, finally, three kinds of pure crystals have been obtained, respectively.

The phenomenon of cocrystallization is common in alloy and mineral species, but rare in organic matter, especially metal organic compounds,¹ which is mainly because of their complex structures and significant difference in the ground state energies.² Two or more species with different architectures through cocrystallization has gained much attention in the last few years, which is because of their structural diversity and great potential applications.³

Mixed ligands, especially rigid and flexible mixed ligands, were used to construct metal-organic frameworks (MOFs) usually able to get complicated and unusual structures, as functional groups on the ligands offer variable configurations.⁴ $4,4',4''\text{-(nitrilotris(methylene))tribenzoic acid}$ (H_3L) is a flexible multicarboxylate ligand and has demonstrated excellent coordinating ability, $4,4'\text{-(2,5-dibutoxy-1,4-phenylene)dipyridine}$ (DPDP) is a rigid ligand with flexible butoxy groups (Scheme S1, ESI). We expect to employ these ligands incorporating with cobalt salt to obtain compounds with special structures and function. Although the phenomenon of co-crystallized in one-pot reaction has been reported, most of them are two types of architectures or with the same composition and proportion, only a few examples involving three different structures.⁵ The synthesis of three types of cobalt cores (Co_3 for **1**, Co_2 for **2**, Co_1 for **3**) with different topologies ($\{4^2 \cdot 6\}_2\{4^4 \cdot 6^{10} \cdot 7^9 \cdot 8^5\}$ for **1**, **sql** for **2**, **bnn** for **3**) under the cocrystallization condition has not been reported. Based on different shapes and colors of three kinds of crystals in the initial products, we supposed that they should have best crystallization conditions, respectively. Then we give a quantitative calculation of DFT for these structures, according to the calculation results, by optimizing the synthesis condition, three kinds of one-component crystals have been obtained, respectively (Fig. 1).

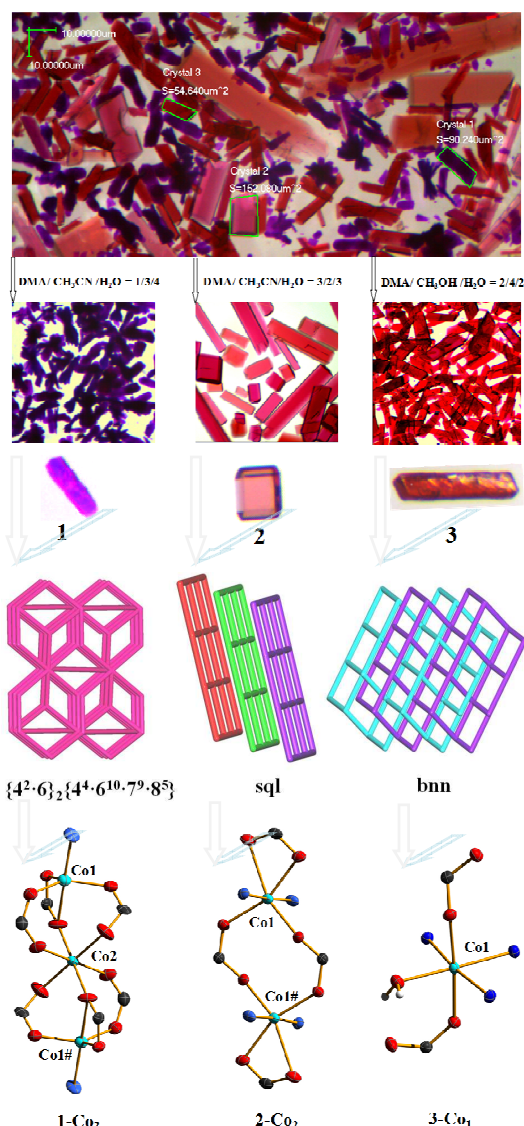


Fig. 1 (top) The optical microscope photographs of complexes **1-3**: complex **1** is purple rice-shaped, **2** is pink block-shaped and **3** is crimson strip-shaped. (middle) Topological representation of complexes **1-3**: $\{4^2 \cdot 6\}_2\{4^4 \cdot 6^{10} \cdot 7^9 \cdot 8^5\}$ for **1**; **sql** for **2**; **bnn** for **3**. (bottom) Different cobalt centers for complexes **1-3**.

55

Single crystal X-ray diffraction study reveals that **1** crystallizes in the monoclinic space group $C2/c$. Its asymmetric unit consists of one and a half Co(II) cations, one L^{3-} anion and half a DPDP ligand (Fig. S2a, ESI). Complex **1** consists of a centrosymmetric trimetallic unit: the central metal ion (Co2) lying on an inversion centre in an octahedral coordination sphere made of six oxygen atoms from six L^{3-} ions; two peripheric cobalt ions (Co1) in a distorted bipyramidal surrounding made of four oxygen atoms from three L^{3-} ions and one DPDP ligand; the Co1...Co2 distance is equal to 3.3964(2) Å. Each L^{3-} ion coordinates six metal ions, two carboxylate anions of L^{3-} ion are $\mu_2(\eta_1, \eta_1)$ (O1, O2 and O3, O4) coordination mode and the remaining one $\mu_2(\eta_1, \eta_2)$ mode (O5, O6) (Fig. S2a, ESI). The octahedral coordination sphere of Co2 is slightly distorted as cobalt-oxygen distances are ranging from 1.2025(7) to 2.137(8) Å and the corresponding angles range from 87.1(3)° to 92.9(3)°. These bond lengths are quite similar to those found in trinuclear cobalt unit $[Co_3(CO_2)_6N_2]$.⁶ Six L^{3-} ligands linked the centrosymmetric trinuclear cobalt unit into an open hexagonal ring, the DPDP ligands coordinate Co(II) ions from up and down positions of the ring (Fig. S2b and S2c, ESI). If don't consider the linear ligand DPDP, the framework constructed from L^{3-} ligands and trimetallic units can be regarded as a 3,6-c net **flu-3,6-C2/c** topology (with the point symbol $\{4^2 \cdot 6\}_2 \{4^4 \cdot 6^2 \cdot 8^7 \cdot 10^2\}$). When the linear ligands are taken into account, we get a new topology with the point symbol of $\{4^2 \cdot 6\}_2 \{4^4 \cdot 6^{10} \cdot 7^9 \cdot 8^5\}$ (Fig. S2f, ESI)

The asymmetric unit of **2** consists of one Co(II) cation, one HL^{2-} anion and one DPDP ligand (Fig. S3a, ESI), which crystallizes in the triclinic space group $P\bar{1}$. Complex **2** consists of a centrosymmetric dinuclear cobalt center: each Co(II) ion is six-coordinated by four carboxylic oxygen atoms from three symmetrical HL^{2-} ligands at the equatorial positions and two nitrogen atoms from two symmetrical DPDP ligands at the axial position; the Co1...Co1# distance is equal to 4.5530(11) Å. Two deprotonated carboxylate groups of H_3L ligand adopt different coordination modes, one takes the bisonodentate coordination mode to bridge two Co centers while the other adopts chelating in a bidentate mode. As shown in Fig. S3b(ESI), pairs of symmetry-related HL^{2-} ligands adopt a bridging mode joining adjacent Co(II) cations to form an infinite 1D double chain, which contains eight-membered and thirty-two-membered rings. Then, such chains are further linked by DPDP ligands to form a 2D network. If the dinuclear SBUs $[Co_2(CO_2)_2]$ are considered as 4-connected nodes, and all crystallographically independent ligands are considered as linkers; thus, the 2D network can be simplified to an **sql** net with point symbol $\{4^4 \cdot 6^2\}$ (Fig. S3c, ESI).

Unlike **1** and **2**, complex **3** is a mononuclear structure, its asymmetric unit contains one Co(II) cation, one HL^{2-} anion, one and a half DPDP ligands, one coordinated water molecule and one free water molecule (Fig. S4a, ESI). The local coordination geometry around the Co^{2+} ion can be described as a $\{CoN_3O_3\}$ distorted octahedron, with the axial positions occupied by two oxygen atoms from two HL^{2-} ligands. Its equatorial plane consists of three N donor atoms from three DPDP ligands and one oxygen atoms from one coordinated water molecule. The DPDP linkers and Co^{2+} ions forms a 2D layered structure (Fig. S4b, ESI). Such layers are further connected by HL^{2-} ligands, leading to the formation of a 3D framework. The Co^{2+} ion can be regarded as a

five-connected node, the HL^{2-} anion and each DPDP ligand can be considered as a linear linker; thus the network is topologically classified as a uninodal 2-fold interpenetrating net with the **bnm** [hexagonal boron nitride] topology and one unique tile $[4^6 \cdot 6^4]$ (Fig. S4c, ESI).

Because of the presence of three different cobalt centers in complexes **1-3**, we focused on their magnetic behavior. Variable-temperature direct-current (dc) magnetic susceptibility measurements for the solid powdered samples of **1-3** were carried out in the temperature range 1.8-300 K under an applied field of 100 Oe for **1** (2000 Oe for **2**, 1000 Oe for **3**). The $\chi_M T$ versus T plot is shown in Figure 2(a) for the $Co^{II}Co^{II}Co^{II}$ system $[d^7 (S = 3/2) - d^7 (S = 3/2) - d^7 (S = 3/2)]$ of **1**. At room temperature, the $\chi_M T$ value is $7.81 \text{ cm}^3 \text{ mol}^{-1} \text{ K}$, which is greater higher than that expected for three high-spin Co^{II} ions through the spin only formula ($3 \times 1.875 = 5.625 \text{ cm}^3 \text{ mol}^{-1} \text{ K}$ with $g = 2.0$). It could be due to the occurrence of an unquenched orbital contribution typical of the $^4T_{1g}$ ground state for octahedral high-spin Co^{II} complexes.^{7,8} Upon lowering the temperature, the $\chi_M T$ product

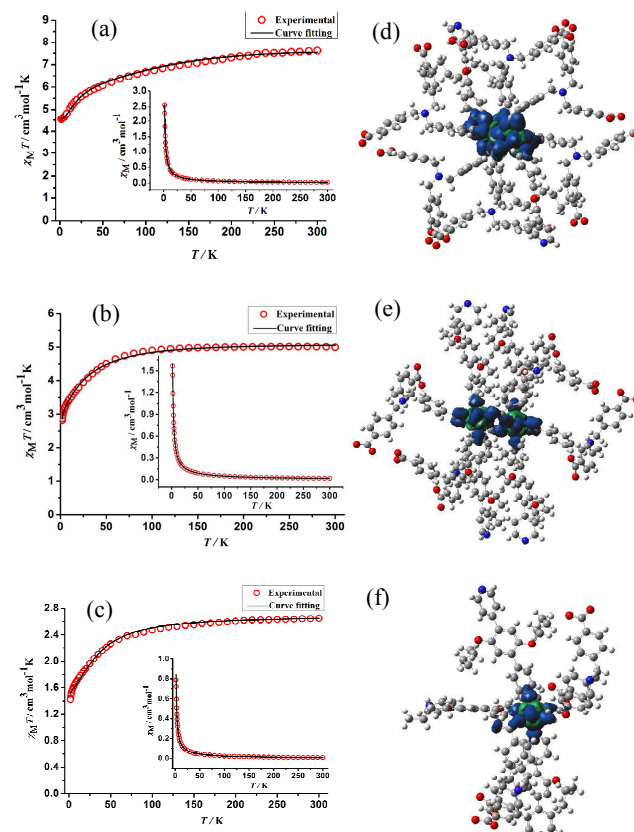


Fig. 2 (left) Temperature dependence of the $\chi_M T$ product (a) for **1**, (b) for **2**, (c) for **3**; χ_M vs. T plot at different temperatures is presented in an inset. (right) Spin densities of (d) **1**, (e) **2**, (f) **3**, calculated at the B3LYP/LANL2DZ level.

decreases gradually to about 50 K, and then it rapidly drop and reach a minimum value of $6.77 \text{ cm}^3 \text{ mol}^{-1} \text{ K}$ at 1.8 K. The temperature-dependent magnetic susceptibility was fitting using the PHI program⁹ by the spin Hamiltonian given in eq 1 (ESI). In this model, the magnetic interaction between the terminal Co^{II} centers (6.793 Å apart) could be neglected $[H = -\{J_{12}(S_1 S_2) +$

$J_{23}(S_2S_3) + J_{13}(S_1S_3)$, the terminal Co^{II} ions $J_{13} = 0$.¹⁰ Initially, no reasonable fitting data was obtained, when the single-ion magnetic anisotropies of the three Co^{II} ions were not considered. Hence, the magnetic anisotropies are assumed to be axial (D_1 , D_2 and D_3). Considering the identical of Co^{II}(1) and Co^{II}(3) sites, D_1 and D_3 were fixed to the equivalent value. A good fit to the data can be obtained: $J = +0.034 \text{ cm}^{-1}$, $D_{1,3} = -22.1 \text{ cm}^{-1}$, $D_2 = 18.5 \text{ cm}^{-1}$, $g = 2.06$. The positive and very small value of the exchange parameter J suggests the weak ferromagnetic intra-complex magnetic interaction in this molecular, which is in agreement with other reported polynuclear Co^{II} complexes.¹¹ The $\chi_M T$ versus T plot of **2** is shown in Figure 2(b), as the temperature cools, $\chi_M T$ continuously decreases from $5.01 \text{ cm}^3 \text{ mol}^{-1} \text{ K}$ at 300 K to $2.78 \text{ cm}^3 \text{ mol}^{-1} \text{ K}$ at 1.8 K. The value of $\chi_M T$ at 300 K is greater than the expected value for high-spin Co^{II} ions through the spin only formula ($2 \times 1.875 = 3.75 \text{ cm}^3 \text{ mol}^{-1} \text{ K}$ with $g = 2.0$). For **3**, as seen in Figure 2(c), the value of $\chi_M T$ at 300 K is $2.65 \text{ cm}^3 \text{ mol}^{-1} \text{ K}$, which is also greater than the value $1.875 \text{ cm}^3 \text{ mol}^{-1} \text{ K}$ for one isolated high-spin Co(II) ions. The magnetic susceptibilities of **2** and **3** can be fitted well by the PHI program though the spin Hamiltonian given in eq 2 for **2**, eq 3 for **3** (ESI), with $J = -0.044 \text{ cm}^{-1}$, $D_1 = D_2 = 21.104 \text{ cm}^{-1}$, $g = 2.33$ for **2**, and $D = +35.18 \text{ cm}^{-1}$, $E = -1.12 \text{ cm}^{-1}$, $g_x = g_y = 2.25$, $g_z = 2.67$ for **3**. The negative and small value of the exchange parameter J for **2** suggests the weak antiferromagnetic interaction between Co ions. The spin density distributions on three different cobalt centers clearly show the number of single electron, as seen in Figure 2(d)-(f), which is also indicated the high-spin Co^{II} ions in **1-3**.

The relative thermodynamic stabilities of cocrystallization were investigated through quantum chemical calculations of these systems on the basis of experimental crystal structures (Fig. S16, ESI). The detailed information is listed in the Supporting Information. DFT ground state energies and the gaps of frontier molecular orbital energy for three different structures are listed in Table S3 and Figure S17. It is shown that both the total energies and gap values are close for **1** and **2**, but different from **3**. The binding energies are -0.94 for **1**, -2.00 for **2**, -1.38 for **3** ($\times 10^4$ kcal/mol) (Tab. S3, ESI). From these thermodynamic data, it is understandable that all the three Co-MOFs could be stable under certain conditions, but a minor altered external factor will be a challenge for crystallizing independently between **1** and **2**.¹²

Based on the above discussion, we have optimized the conditions of crystallization to purify three kinds of crystals respectively. The relative studies were conducted and observations are detailed in Table S4 (ESI): (1) when DMA/CH₃OH is used as solvent systems, the ratio is 3/5 (means 3 ml vs. 5 ml), temperature is set at 95 °C, complexes **1**, **2** and **3** with proportions about 1 : 2 : 2 were obtained (Fig. S1, ESI). When the ratio changes from 1/7 to 2/6 or pure CH₃OH, a lot of impurities appeared; from 4/4 to 7/1 or pure DMA, the amount of crystals gradually reduced, until clear solution. When DMA is replaced by DMF, the phenomenon is almost the same. (2) When DMA/CH₃CN was used as the solvent system, the ratio from 5/3 to 6/2, two-component crystals **1** and **2** were obtained (Fig. S18, ESI). When CH₃CN is replaced by H₂O, the absolute two-component crystals **2** and **3** were obtained in the ratio 3/5 (Fig. S19, ESI), **1** and **3** were obtained in the ratio 6/2 (Fig. S20, ESI). Here, we have yet to obtain one-component crystals, and then we

try to use the three-component solvent instead of two-component solvent systems. (3) When DMA/CH₃OH/H₂O is used as solvent systems, the ratio is 2/4/2, many one-component crystals **3** were obtained (Fig. S21, ESI). When CH₃OH is replaced by CH₃CN, a few one-component crystals **1** were obtained in the ratio 1/3/4 (Fig. S22, ESI), **2** was obtained in the ratio 3/2/3 (Fig. S23, ESI).

All above optimizational experiments were carried out at 95 °C with total amount of solvent of 8.0 ml. From Table S4, in the absence of DMF or DMA in solvent systems, only powder was generated. Nevertheless, if the solvent system is only DMF or DMA, clear solution will be generated. In most cases, we get the mixed components, or the components contain impurities. Unlike **3**, one-component crystals **1** or **2** only exist within a very small range, direct cause is the polarity and solubility of the solvents, actually, it is the result of the combination of dynamics and thermodynamics. The phenomenon that selected solvent systems play important role on the synthesis of complexes has been observed in the MOF area.¹³

In summary, three different Co-MOFs (Co₃ for **1**, Co₂ for **2**, Co₁ for **3**) with different topologies have been co-crystallized in one-pot crystallization. From the proportion of three species in the initial products, through quantum chemical calculations of these systems, we try our best to optimize the synthesis conditions, finally, three kinds of one-component crystals have been obtained.

This work was supported by grants from the Natural Science Foundation of China (No. 21371092, 91022011) and National Basic Research Program of China (2010CB923303).

Notes and references

^a State Key Laboratory of Coordination Chemistry and ^b Institute of Theoretical and Computational Chemistry, School of Chemistry and Chemical Engineering, Collaborative Innovation Center of Advanced Microstructures, Nanjing University, Nanjing, 210093, P. R. China. Fax: (+86)25-83314502; E-mail: zhenghg@nju.edu.cn
Electronic supplementary information (ESI) available: IR, PXRD, TG, computational methods, optimization experiment, the selected bond lengths and angles. CCDC 1040508–1040510. For ESI and crystallographic data in CIF or other electronic format see DOI: 10.1039/b000000x/

- (a) H. Yang, Z. M. Wang, H. X. Jin, B. Hong, Z. Y. Liu, C. M. Beavers, M. M. Olmstead and A. L. Balch, *Inorg. Chem.*, 2013, **52**, 1275; (b) J. Shin, N. H. Ahn, M. A. Cambor, C. M. Zicovich-Wilson and S. B. Hong, *Chem. Mater.*, 2014, **26**, 3361.
- (a) Y. Liu, N. Li, L. Li, H. L. Guo, X. F. Wang and Z. X. Li, *CrystEngComm*, 2012, **14**, 2080; (b) M. H. Mir, S. Kitagawa and J. J. Vittal, *Inorg. Chem.*, 2008, **47**, 7728.
- (a) R. S. Winter, J. M. Cameron and L. Cronin, *J. Am. Chem. Soc.*, 2014, **136**, 12753; (b) J. P. Zhang and X. M. Chen, *Chem. Commun.*, 2006, 1689; (c) J. P. Zhang, S. L. Zheng, X. C. Huang and X. M. Chen, *Angew. Chem., Int. Ed.*, 2004, **43**, 206; (d) K. M. Fromm, J. L. S. Doimeadios and A. Y. Robin, *Chem. Commun.*, 2005, 4548.
- (a) Y. X. Hu, H. B. Ma, B. Zheng, W. W. Zhang, S. C. Xiang, L. Zhai, L. F. Wang, B. L. Chen, X. M. Ren and J. F. Bai, *Inorg. Chem.*, 2012, **51**, 7066; (b) K. T. Butler, C. H. Hendon and A. Walsh, *J. Am. Chem. Soc.*, 2014, **136**, 2703.
- (a) J. S. Hu, L. Qin, M. D. Zhang, X. Q. Yao, Y. Z. Li, Z. J. Guo, H. G. Zheng and Z. L. Xue, *Chem. Commun.*, 2012, **48**, 681.
- (a) K. S. Gavrilenko, S. V. Punin, O. Cador, S. Golhen, L. Ouahab and V. V. Pavlishchuk, *J. Am. Chem. Soc.*, 2005, **127**, 12246; (b) S. G. Konstantin, L. G. Yann, C. Olivier, G. Stéphane and O. Lahcène, *Chem. Commun.*, 2007, 280; (c) A. K. Sharma, F. Lloret, and R. Mukherjee, *Inorg. Chem.*, 2013, **52**, 4825.

-
- 7 (a) B. N. Figgis, M. Gerloch, J. Lewis, F. E. Mabbs, G. A. Webb, *J. Chem. Soc. A*, 1968, 2086; (b) M. Gerloch, P. N. Quedstedt, *J. Chem. Soc. A*, 1971, 3729.
- 8 F. E. Mabbs, D. J. Machin, *Magnetism in Transition Metal Complexes*, Chapman and Hall: London, 1973.
- 9 F. C. Nicholas, P. A. Russell, D. T. Lincoln, S. Alessandro and S. M. Keith, *J. Comput. Chem.*, 2013, **34**, 1164.
- 10 Q. Zhao, H. Li, Z. Chen, R. Fang, *Inorg. Chim. Acta*, 2002, **336**, 142.
- 11 (a) V. Mishra, F. Lloret, R. Mukherjee, *Inorg. Chim. Acta*, 2006, **359**, 4053; (b) F. Lloret, M. Julve, J. Cano, R. Ruiz-Garcia, E. Pardo, *Inorg. Chim. Acta*, 2008, **361**, 3432.
- 12 Y. X. Hu, H. B. Ma, B. Zheng, W. W. Zhang, S. C. Xiang, L. Zhai, L. F. Wang, B. L. Chen, X. M. Ren, J. F. Bai, *Inorg. Chem.*, 2012, **51**, 7066.
- 15 13. (a) J. Zhang, T. Wu, S. M. Chen, P. Y. Feng, X. H. Bu, *Angew. Chem., Int. Ed.*, 2009, **48**, 3486; (b) Y. Kang, S. M. Chen, F. Wang, J. Zhang, X. H. Bu, *Chem. Commun.*, 2011, **47**, 4950.